C.1.c.2.5-Competitive Removal of Cationic Dye Using NiAl-LDH.pdf

By Risfidian Mohadi

EEET ECOLOGICAL ENGINEERING & ENVIRONMENTAL TECHNOLOGY

Ecological Engineering & Environmental Technology 2021, 22(4), 124–135
https://doi.org/10.12912/27197050/138120
ISSN 2719-7050, License CC-BY 4.0

Received: 2021.04.22
Accepted: 2021.05.15
Published: 2021.06.07

Competitive Removal of Cationic Dye Using NiAl-LDH Modified with Hydrochar

Normah[1], Neza Rahayu Palapa[3], Tarmizi Taher[2,5], Risfidian Mohadi[5], Fitri Suryani Arsyad[4], Aldi Priambodo[5], Aldes Lesbani[3,5*]

[1] Master Programme Graduate School of Mathematics and Natural Sciences, Sriwijaya University, Jl. Padang Selasa No. 524 Ilir Barat 1, Palembang-South Sumatra, Indonesia
[2] Departement of Environmental Engineering, Faculty of Mathematics and Natural Sciences, Insitut Teknologi Sumatera, Jl. Terusan Ryacudu, Way Hui, Jati Agung, Lampung, Indonesia
[3] Graduate School of Mathematics and Natural Sciences, Sriwijaya University, Jl. Padang Selasa No. 524 Ilir Barat 1, Palembang-South Sumatra, Indonesia
[4] Department of Physics, Faculty of Mathematics and Natural Sciences, Sriwijaya University, Jl. Palembang-Prabumulih, Km. 32, Ogan Ilir, South Sumatra, Indonesia
[5] Research Center of Inorganic Materials and Coordination Complexes, Faculty of Mathematics and Natural Sciences, Universitas Sriwijaya, Jl. Palembang Prabumulih, Km. 32, Ogan Ilir, Indonesia
* Corresponding author's email: aldeslesbani@pps.unsri.ac.id

ABSTRACT

In this study, NiAl-LDH was modified with hydrochar using the NiAl-Hydrochar composite coprecipitation method. Materials were characterized by XRD and FT-IR analysis. XRD diffractogram and FT-IR spectra show that the NiAl-Hydrochar composite material has the characteristics of the precursors. NiAl- Hydrochar composite materials have a large adsorption capacity to adsorb cationic dyes. The adsorption follows the Langmuir adsorption isotherm model with the maximum capacity (Q_{max}) of the NiAl-Hydrochar composite material reaching 256.410 mg/g for malachite green and the adsorption process takes place spontaneously and endothermically. The regeneration process of NiAl-Hydrochar composites was more stable and the decrease was not significant (>70%). The selectivity of the dye mixture showed that the adsorbent was more selective for malachite green dye compared to methylene blue and rhodamine-B.

Keyword: layered double hydroxide, composite, hydrochar, cationic dye, stability, selectivity

INTRODUCTION

Among the environmental problems that often occur, the handling of dye wastewater is still one of the most discussed and is of concern to the world (Mrózek et al., 2019; Stawiński et al., 2018). Dyes are pollutants produced in various industries and often in heavy metals in wastewater (Stawiński et al., 2018). Many dyes have wide applications in various textile industries (Daud et al., 2019), cosmetics, plastics (Jiang et al., 2019), paints, and paper (Saghir et al., 2020). These pollutants have harmful effects on living organisms and are resistant to conventional treatments because of their carcinogenic and mutagenic properties (Daud et al., 2019; Stawiński et al., 2018). Several technologies for dye removal have been developed including membrane treatment, coagulation or flocculation (Daud et al., 2019), adsorption (Palapa et al., 2020), ion exchange (Mikif et al., 2018), manipulation and photodegradation (Saghir et al., 2020). Technologies for removing pollutants have improved (Stawiński et al., 2018).

Adsorption-based industrial wastewater treatment has received considerable attention during

the last two decades (Mrózek et al., 2019). Adsorption is considered one of the best industrial wastewater treatment methods because it is more efficient, broad application, ease of operation (Kaykhaii et al., 2018), insensibility to toxicants (Stawiński et al., 2018) and adjustable adsorption selectivity (Mrózek et al., 2019). Thus, finding new adsorbents with sufficient affinity to address dye waste is a scientific and industrial challenge (Mrózek et al., 2019)

Layered double hydroxide (LDHs) known as anionic clays, are 2D structured layered materials with controlled structure and composition and have excellent absorbent properties (Wang & Zhang, 2020). LDHs chemical formula is $[M^{2+}1\text{-}xM^{3+}x\ (OH)_2]^{x+}\ [A^{n-}_{x/n}.mH_2O]$, where M^{2+} is divalent and M^{3+} trivalent metal ions and A^n represent the anions between layers (Saghir et al., 2020). Layered double hydroxide as a classic lamellar metal hydroxide that accommodates anions in its interlayer (Jiang et al., 2019), has high porosity (Siregar et al 2021), high surface area (Shan et al., 2014) is a promising adsorbent candidate. The application of LDH as an adsorbent has disadvantages such as in the adsorption regeneration process because LDH can peel off the layer during the application process so that it can be used repeatedly (Palapa et al., 2020). Therefore, it is more effective if it is modified to form a composite with the supporting material to increase the integrity of the coating. Supporting materials that can be used are carbon-based materials such as activated carbon (Hu et al., 2020), graphite (Lv et al., 2019), biochar (Li et al., 2020) and hydrochar (He et al., 2019).

Hydrochar has a porous structure and functional groups which can be ideal support material for LDH. LDH composites with carbon-based support materials can effectively prevent agglomeration, increase the surface area to provide more active sites to improve the adsorption performance (Hu et al., 2020). According to Zhang et al. (2014) LDH was modified with carbon-based materials such as hydrochar. Almoisheer et al. (2019) reported that the synthesis of CuAl-LDH/carbon nanotubes for indigo carmine (IC) organic dyes from aqueous solutions has a maximum adsorption capacity of 294.117 mg/g at 20 °C. Research Rathee et al. (2019) the ability of the NiFe/Ti material to be applied as an adsorbent to remove anionic dyes with a maximum adsorption capacity for methyl orange of 32.616 mg/g, congo red of 29.970 mg/g, methyl blue of 29.940 mg/g and orange G of 39.952 mg/g. Based on research by Alagha et al. (2020) reported that the biochar-Mg/Al composite has the potential to be used repeatedly in the phosphate adsorption process and the regeneration process has decreased which is not too significant after five cycles of 92%. Ahmed et al. (2020) reported that MgFe-LDH/waste foundry sand composites have work stability with six times recycling with an efficiency exceeding 80% to remove congo red.

In this study, NiAl-LDH was synthesized using the coprecipitation method modified with hydrochar (HR) to produce a NiAl-HR composite. The material is used as an adsorbent to remove contaminants from malachite green (MG), methylene blue (MB) and rhodamine-B (Rh-B). The materials were analyzed using XRD, FT-IR characterization. Application as an adsorbent, this research carries out an adsorption process with isotherm and thermodynamic parameters, studies of regeneration and adsorption selectivity.

EXPERIMENT

Chemicals and instrumentations

All reagent and chemicals used were analytical grades supplied by Merck and Sigma-Aldrich including $Ni(NO_3)_2{\cdot}6H_2O$ (99%) and $Al(NO_3)_3{\cdot}9H_2O$ (99%) and used as the precursors for NiAl-LDH, NaOH (99%), and HCl (37%) were used without further purification. Deionized (DI) water was used for all synthesis and treatment processes. In this experiment, the biomass of rambutan fruit peel (*Nephelium lappaceum L.*) was collected from household waste as a precursor for the hydrochar manufacturing process using the hydrothermal carbonization method. Before being carried out for the hydrothermal carbonization process, the samples were dried at a temperature of 100°C to remove moisture.

Synthesis of NiAl-LDH

NiAl-LDH was prepared by the coprecipitation method (Lesbani et al., 2020). The molar ratio used for the 3:1 LDH synthesis from a mixed solution with $Ni(NO_3)_2{\cdot}6H_2O$ 3 M and $Al(NO_3)_3{\cdot}9H_2O$ 1 M is added to the beaker. The mixture was stirred for 30 minutes and then slowly dripped with 2M NaOH to pH 10. Then,

stirred for 12 hours at a temperature of 60°C. After that, the samples were dried at 100°C in an oven for 12 hours.

Preparation hydrochar

Hydrothermal carbonization was performed using a 100 mL hydrothermal apparatus. 2.5 grams of rambutan (*Nephelium lappaceum* L.) rind powder then put into Teflon and added with 50 mL of deionized water which will be used for the carbonization process. Then, the Teflon was put into the autoclave, tightly closed, and heated in an oven with a temperature of 200°C for 10 hours. The solid product is separated from the liquid product by filtration and the solid is dried for 12 hours at a temperature of 150°C. black solids as a result of the hydrothermal carbonization process are called hydrocarbons.

Preparation composite NiAl-HR

Synthesis of NiAl-HC composites was carried out using the coprecipitation method. 10 mL of $Ni(NO_3)_2 \cdot 6H_2O$ 3 M was mixed with 10 mL of $Al(NO_3)_3 \cdot 9H_2O$ 0.25 M and stirred. Then, 1 g of solid hydrochar is added (Palapa, Taher, Rahayu, et al., 2020). The mixture is dripped with 2 M NaOH until it reaches pH 10 slowly. The mixture was stirred for 3 days at 80°C. The resulting solid was filtered, washed, and dried at 60°C for 1 day.

Characterization methods

X-ray diffraction (XRD) data from NiAl-LDH, HC and Composite NiAl-HC materials between 5 and 80 using XRD Rigaku miniflex-6000 using Cu K radiation at a scanning rate of 1 s^{-1} was used to determine the phase structure of LDH samples. Observation of functional groups of the material used analysis with the FT-IR Shimadzu Prestige-2 which was measured with a wavenumber range of 400–4000 cm^{-1} and using KBr pellets. Morphological observations were carried out with a scanning electron microscope (SEM) Quanta-650 Oxford instrument at an acceleration voltage of 10 kV. Analyzing the concentration of adsorbed dye using the BK-UV Biobase BK-UV 1800 PC spectrophotometer with long wavelengths of rhodamine-B (560 nm), malachite green (617 nm), and methylene blue (664 nm).

Adsorption isotherm

The adsorption equilibrium experiment was carried out in a 100 mL beaker, in which 50 mL of dye solution with different initial concentration variations (20, 40, 60, 80 and 100 mg/L) were added to the beaker. 0.05 g of adsorbent was added to the dye solution and stirred for 2 hours with various adsorption temperatures (303, 313, 323 and 333K) to achieve the adsorption equilibrium. then the final concentration of the dye in the solution was analyzed using a spectrophotometer at each wavelength. The sample should be separated between the filtrate and the residue before analysis to minimize the fine disturbance of the adsorbent during analysis.

The isotherm parameters are obtained from the Langmuir and Freundlich equations. Langmuir and Freundlich isotherm equations are as follows:

Langmuir: $$\frac{C}{m} = \frac{1}{bKML} + \frac{C}{b} \quad (1)$$

Freundlich: $$\text{Log } q_e = \log K_F + 1/n \log C_e \quad (2)$$

where: C is a saturated concentration of adsorbate; m is the amount of adsorbate; b is the maximum adsorption capacity ($mg.g^{-1}$); K_M is the Langmuir constant ($L.mg^{-1}$). q_e is adsorption capacity at equilibrium ($mg.g^{-1}$); C_e is a concentration of adsorbate at equilibrium ($mg.L^{-1}$); K_F is Freundlich constant.

Thermodynamic parameters are calculated by equations 3 and 4:

$$\ln K_{eq} = \frac{\Delta S}{R} - \frac{\Delta H}{RT} \quad (3)$$

$$\Delta G = \Delta H - T\Delta S \quad (4)$$

where: T is temperature (K), R is the gas constant (8.314 $J.mol^{-1}.K^{-1}$), K_{eq} the reaction on charge temperature, ΔG is the change in Gibbs free energy (kJ/mol), ΔS is the change in entropy (kJ/mol), and ΔH is the change in entropy (kJ/mol).

Regeneration experiment

Regeneration was carried out using an ultrasonic instrument which was carried out by adsorbing 50 mL of the dye solution with a concentration of 100 mg/L, plus 0.5 g of adsorbent and stirring for 4 hours. After the adsorption process is carried out, the desorption process is carried out using water. The desorption process is carried out with the adsorbent that has been used

for adsorption and taken as much as 0.01 g, each adding 10 mL of water and stirring for 2 hours. The regeneration process uses used adsorbents. The solution was measured and analyzed using a UV-Vis spectrophotometer. Before being analyzed with a UV-Vis spectrophotometer, the mixture must be separated between the filtrate and the residue. The regeneration process is carried out in seven cycles with the same procedure as before.

Selectivity adsorption

The selectivity was done by mixing three dyes, namely malachite green, methylene blue and rhodamine-B using a concentration of 10 mg/L as much as 100 mL. The mixture is then added 0.05 g of adsorbent in 50 mL of the dye mixture and stirred with time variations of 0, 15, 30, 60 and 120 minutes. Then separate the filtrate and residue, the filtrate was measured for wavelength with a UV-Vis spectrophotometer.

RESULTS AND DISCUSSION

XRD analysis aims to analyze the structure of the material that has been synthesized. The NiAl-LDH, HC, NiAl-HC diffraction patterns are presented in Figure 1. The NiAl-LDH diffraction pattern in Figure 1 (a) shows the main diffraction peaks that are often used to identify good crystallinity of LDH structures at 2θ = 11.03°, 22.7°, 35.0°, 62.8°, and 63.1° are assigned to reflection (003), (006), (012), (110) and (113) respectively (Tcheumi et al., 2020). According to Oliveira et al. (2016) the XRD diffraction pattern of hydorchar in Figure 1(b) shows that HC with a peak of 2θ = 22° with a diffraction plane (002) represents cellulose I and a peak between 15° to cellulose II with a diffraction plane (101) which has an amorphous form. Figure 1(c) shows the NiAl-HC composite pattern which has the same diffraction pattern as NiAl-LDH and HC with a diffraction angle of 11.03° and HC at a diffraction angle of 22°. The diffraction pattern of NiAl-HC composites decreased in intensity due to the amorphous HC.

Figure 2(a) shows the FT-IR spectrum of NiAl-LDH. The vibratory band at 3483 cm^{-1} corresponds to the strain vibrational mode of the water molecules which are fissured by hydrogen bonds. Likewise, bands approaching 1630 cm^{-1} correspond to the bending vibrations of O-H from the water interlayer. The intense band at 1384 cm^{-1} is caused by the vibration mode of the nitrate ion in the interlayer space. The band characteristics in the metal-oxygen bond stretching appear at 664 cm^{-1} and 540 cm^{-1} due to the various lattice vibrations associated with the sheet metal hydroxide (Tcheumi et al., 2020). Figure 2(b). shows the main infrared absorption band of HC. The FT-IR spectrum is derived from cellulose and hemicellulose. It has been observed that the band between 3425 cm^{-1} is associated with the strain of the O-H groups forming hydrogen bonds and the types of intramolecular and intermolecular bonds that occur in polymer compounds, such as phenols, alcohols, carboxylates. acids, such as cellulose, hemicellulose, and lignin. The weak band at 2924 cm^{-1}, in HC, is a bond related to the -CH strain indicating the presence of lignin in HC. The 1620 cm^{-1} band indicates the presence of an aromatic

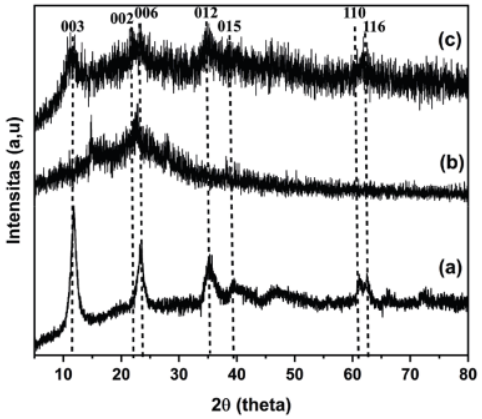

Figure 1. XRD powder patterns of NiAl-LDH (a), HR (b), NiAl-HR (c)

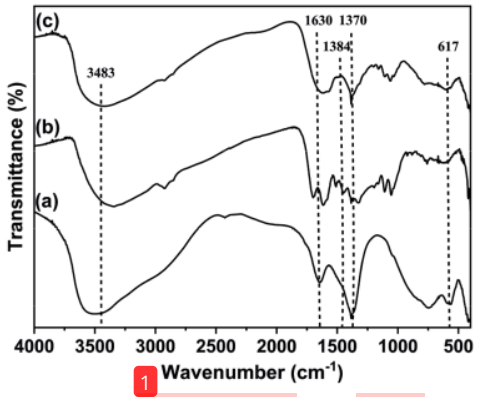

Figure 2. FTIR spectrum of NiAl-LDH (a), HR (b), NiAl-HR (c)

C=C group. The band at 1059 cm^{-1} comes from the hemicellulose C-O bonds. Figure 2(c) shows the spectrum of the NiAl-HR composite. The peaks appeared at 3483 cm^{-1}, 1630 cm^{-1}, 1384 cm^{-1} and 617 cm^{-1}. All the peaks that appeared in the NiAl-HR composites were NiAl-LDH and HR vibrations.

The thermodynamic parameters were studied by varying the initial concentrations of malachite green, methylene blue, and rhodamine-b with the adsorption temperature as shown in Figure 3, Figure 4 and Figure 5. The figure shows that the adsorption capacity increases with increasing the adsorption temperature used. It is very visible that temperature greatly affects the adsorption capacity of the dye, this is because when the temperature increases it can cause an increase in the number of active sites and there will be an increase in the number of interactions between adsorbates. and active sites. by increasing the number of interactions between the adsorbate and the active site, it will increase the amount of adsorption capacity.

Table 1 shows that the highest adsorption capacity (Q_{max}) in NiAl-HR composite material reached 256.410 mg/g at 333 K for malachite green, methylene blue of 144.928 mg/g, and Rhodamine-B of 71.429 mg/g. So that the LDH material which is composed with Hidrochar is considered as an effective adsorbent to remove cationic dyes. Adsorption Capacity NiAl-HR has a greater adsorption capacity compared to pure materials. The adsorption capacity of NiAl-HR to adsorb MG was greater than that of MB and Rh-B.

The determination of the adsorption isotherm model is seen from the linear regression value which is close to the value 1. From the data in Table 1, it can be seen that the isotherm model for each adsorbent and adsorbate tends to approach the Langmuir isotherm model with linear

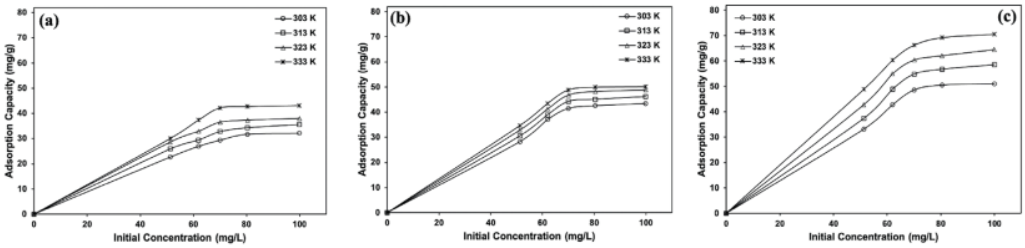

Figure 3. Effect of Malachite Green concentration on NiAl-LDH (a), HR (b), and NiAl-HR (c)

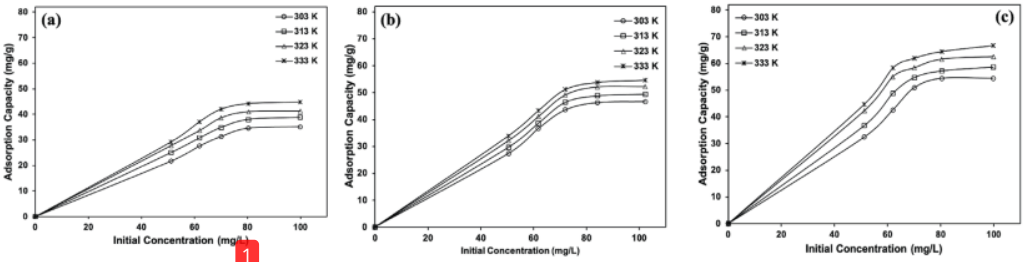

Figure 4. Effect of Methylene Blue concentration on NiAl-LDH (a), HR (b), and NiAl-HR (c)

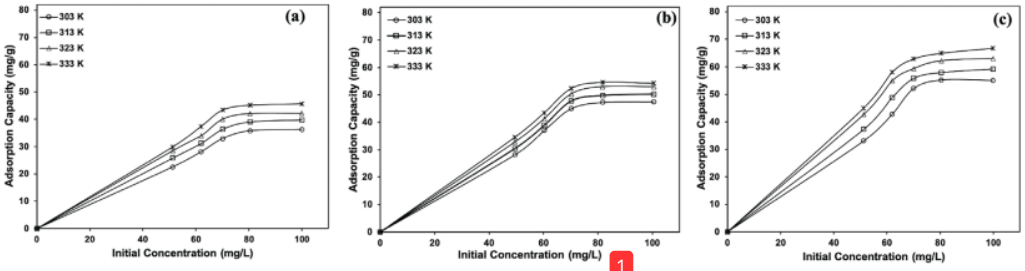

Figure 5. Effect of Rhodamine-B concentration on NiAl-LDH (a), HR (b), and NiAl-HR (c)

Table 1. Isotherm model of Malachite Green, Methylene blue and Rhodamine-B adsorption on NiAl-LDH, HR and NiAl-HR

Adsorbate	Adsorben	Langmuir			Freundlich		
		Qm(mg/g)	kL	R^2	n	kF	R_2
MG	NiAl-LDH	95.238	0.029	0.997	1.576	2.756	0.973
	HR	99.010	0.090	0.994	15.361	35.392	0.940
	NiAl-HR	256.410	0.017	0.999	11.123	3.5675	0.967
MB	NiAl-LDH	74.074	0.067	0.994	2.575	15.559	0.948
	HR	66.225	0.079	0.973	2.404	43.873	0.969
	NiAl-HR	144.928	0.025	0.991	2.699	10.737	0.989
RhB	NiAl-LDH	65.789	0.263	0.990	7.634	13.908	0.916
	HR	68.966	0.048	0.991	1.088	1.766	0.994
	NiAl-HR	71.429	0.089	0.992	0.835	14.224	0.989

regression with a value of $R^2 > 0.997$. According to Hashem et al. (2020), the Langmuir model is based on monolayer adsorption at different active sites, with homogeneous adsorption. According to Dada et al. (2017) Langmuir isotherm model, there is no interaction between adsorbed adjacent species and Hashem et al. (2020) no adsorbate movement in the surface plane. according to Meili et al. (2019) and Elmoubarki et al. (2017). Langmuir model shows adsorption with a uniform energy distribution at the active site and assumes that there are no further interactions between adsorbed molecules. Therefore, Langmuir is considered once the active site is occupied by adsorbate, then no further interactions occur on that site.

Table 2 assumes that the adsorption occurs endothermically because it has a positive H value (10.861–35.221 kJ/mol) and the adsorption process which has an H value <84 kJ/mol, it is assumed that the adsorption process occurs physically. S is positive, assuming the degree of irregularity in the solid-liquid phase during the adsorption process of the dye onto the adsorbent surface (Dang et al., 2020). With this, a positive S value indicates that the dye has a high affinity for the adsorbent because in the adsorption process the energy required to form a bond with the adsorbent is lower than the energy required to break the same bond. According to Neolaka et al. (2020) G is negative, it is assumed that the spontaneity of the adsorption process and the adsorbate has a high affinity for the adsorbent. Decreasing the value of G with increasing adsorption temperature indicates that the adsorption process is better at higher temperatures. It can also be seen from the data that with increasing adsorption temperature, the adsorption concentration of the dye also increases.

The adsorption capacities of several adsorbents for MG, MB and RH-B dyes and the synthesized adsorbents in the form of NiAl-LDH, HR and NiAl-HR used in this study are presented in Table 3. The adsorption capacities of MG, MB and RHB for NiAl-LDH and hydochar have a larger capacity compared to other adsorbents. NiAl-HR composites have a greater adsorption capacity compared to LDH and hydrochar for the adsorption of MG, MB, and Rh-B. This results in the interaction of the hydrochar active site on the composites.

The results of the adsorption regeneration study using NiAl-LDH, HR, and NiAl-HR are shown in Figure 6. The results showed that the NiAl-HR composite material had a greater adsorption capacity and a more stable regeneration process than pure material. The adsorption of malachite green, methylene blue and Rhodamine-B using NiAl-HR material was stable for five regeneration cycles and experienced an insignificant decrease. This is because the process of modifying LDH with carbon-based materials can increase the stability of the structure so that it can be used repeatedly as an adsorbent. Meanwhile, the adsorption of NiAl-LDH and HR experienced a significant decrease in the regeneration process, this was because the material had an unstable structure and peeling and structural damage occurred. So it can be concluded that modification of LDH with hydrochar can increase the stability of the LDH structure for the adsorption regeneration process.

The maximum wavelength of a mixture of malachite green, methylene blue and rhodamine-B dyes was measured in a neutral pH using a UV-Vis spectrophotometer in the wavelength range of

Table 2. Thermodynamic parameters of MG, MB and Rh-B adsorption on NiAl-LDH, HR and NiAl-HR

Dye	Adsorbent	T (K)	Q_e (mg/g)	ΔH (kJ/mol)	ΔS (kJ/mol)	ΔG (kJ/mol)
MG	NiAl-LDH	303	31.748	16.413	0.052	0.523
		313	34.364			-0.001
		323	37.337			-0.525
		333	42.806			-1.050
	HR	303	42.568	10.861	0.037	-0.295
		313	45.065			-0.663
		323	48.276			-1.031
		333	49.941			-1.399
	NiAl-HR	303	50.535	35.221	0.120	-1.173
		313	56.736			-2.374
		323	62.087			-3.575
		333	69.161			-4.776
MB	NiAl-LDH	303	27.611	17.206	0.055	-0.560
		313	30.764			-0.011
		323	33.614			-0.538
		333	37.132			-1.088
	HR	303	46.331	13.766	0.047	-0.452
		313	48.878			-0.921
		323	52.153			-1.391
		333	54.621			-1.860
	NiAl-HR	303	54.457	16.593	0.060	-1.479
		313	57.247			-2.076
		323	61.613			-2.672
		333	64.403			-3.269
Rh-B	NiAl-LDH	303	28.140	17.310	0.056	-0.363
		313	31.220			-0.196
		323	34.005			-0.755
		333	37.441			-1.314
	HR	303	47.275	11.083	0.039	-0.792
		313	49.763			-1.184
		323	52.962			-1.576
		333	54.621			-1.968
	NiAl-HR	303	55.213	17.770	0.065	-1.783
		313	57.938			-2.429
		323	62.204			-3.074
		333	64.929			-3.720

500-700 nm shown in Figure 7. The selectivity of adsorption to the dye mixture can be seen from changes in wavelength the maximum absorbance during adsorption. In neutral conditions, it can be seen that for NiAl-LDH, HR and NiAl-HR adsorbents there is a decrease in absorbance after adsorption. Figure 7 shows that among the mixed dyes, MG dyes were adsorbed more than MB and Rh-B. This can be seen from the decrease in the absorbance value with the adsorption contact time and at 120 minutes the adsorbed concentration of MG reached 50.465 mg/g.

The maximum wavelength of a mixture of malachite green, methylene blue and rhodamine-B dyes was measured in base pH using a UV-Vis spectrophotometer in the 500–700nm wavelength range shown in Figure 8. The selectivity of adsorption to the dye mixture can be seen from changes in wavelength during adsorption. In alkaline conditions, it can be seen that for NiAl-LDH, HR and NiAl-HR adsorbents there is a decrease in absorbance after adsorption. Figure 8 shows that among the mixed dyes, more adsorbed than MB and Rh-B. This can be seen from the decrease in the absorbance value with the adsorption contact time and the adsorbed MG concentration at 120 minutes reached 84.263 mg/g. compared to neutral pH, the adsorbed concentration of alkaline pH is greater.

Table 3. Comparison of several adsorbents to remove MG, MB and Rh-B

Adsorbent	Adsorbate	Adsorption capacity (mg/g)	Reference
Mg/Al LDH	MG	44.444	(Badri et al., 2021a)
Mg-Al/biochar		70.922	(Badri et al., 2021b)
Calcium rich biohar from crab sheel		12.501	(Srivatsav et al., 2020)
ZnAl-Citrate		111	(Hidayati et al., 2020)
NiFe-LDH	MB	23.39	(Elmoubarki et al., 2017)
MgFe-LDH		13.64	(Elmoubarki et al., 2017)
Wet-torrefied microalgal biochar		113	(Srivatsav et al., 2020)
NiAl-LDH		22.989	(Lesbani et al., 2021)
Kaolin	Rh-B	24.704	(Iryani et al., 2020)
Volvariella volvacea		33.51	(Li et al., 2015)
Fe_2O_3		89.3	(Razak & Rohani, 2018)
Surfactant-modified 3D-LDH		52.63	(Zhu et al., 2020)
NiAl-LDH	MG	95.238	This research
HR	MG	99.010	This research
NiAl-HR	MG	256.410	This research
NiAl-LDH	MB	74.074	This research
HR	MB	66.225	This research
NiAl-HR	MB	144.928	This research
NiAl-LDH	Rh-B	65.789	This research
HR	Rh-B	68.966	This research
NiAl-HR	Rh-B	71.429	This research

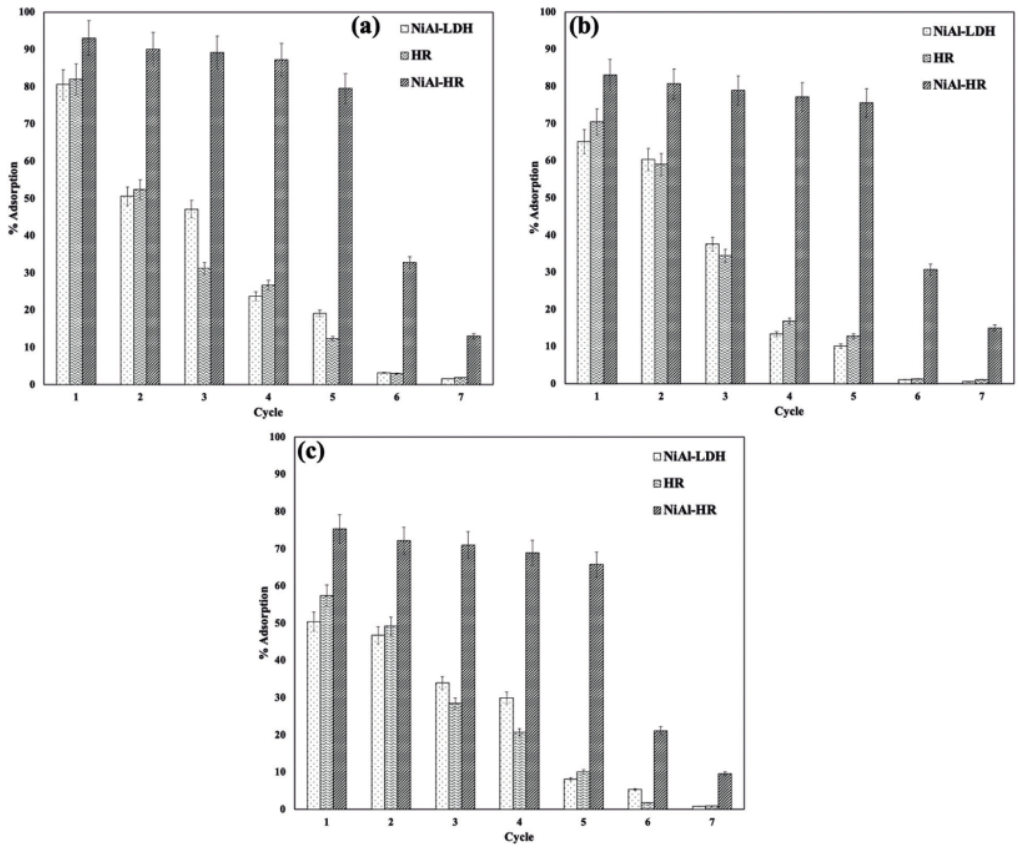

Figure 6. Regeneration MG (a), MB (b) and Rh-B (c) on NiAl-LDH, HR and NiAl-HR

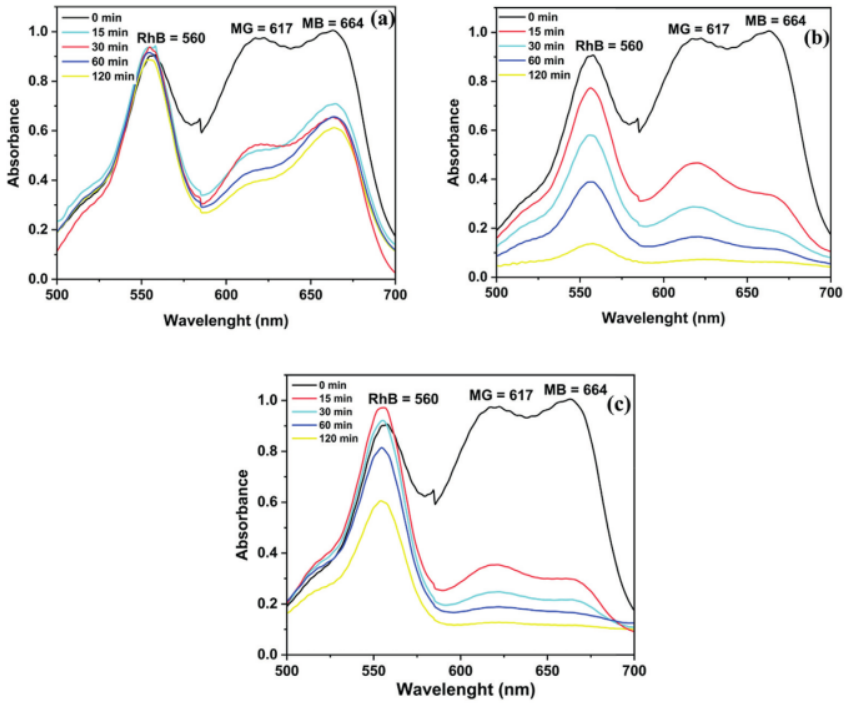

Figure 7. UV-Visible spectra of mixture Mg, MB and Rh-B neutral pH on NiAl-LDH (a), NiAl-HR (b), and HR (c)

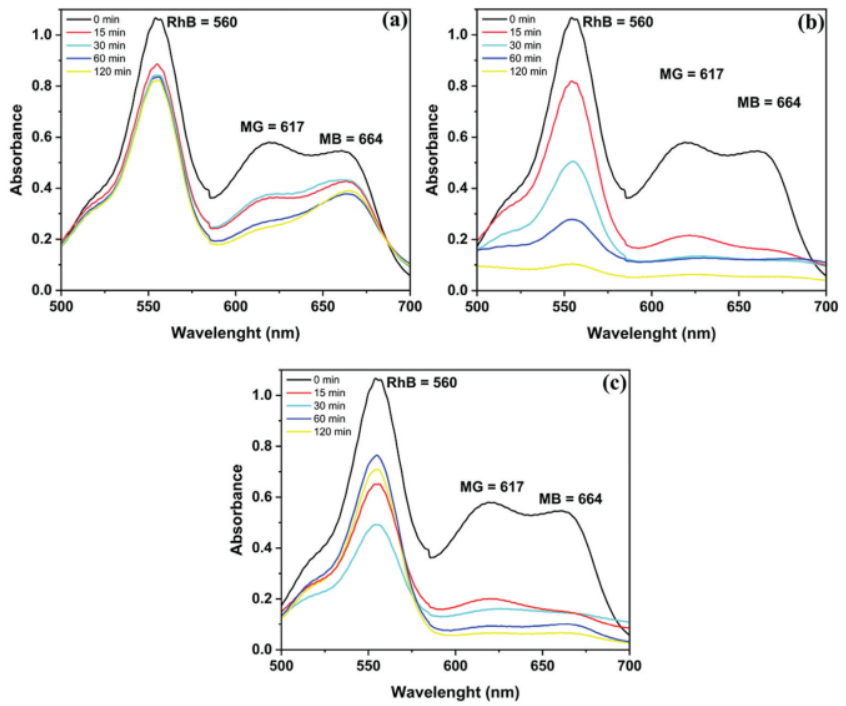

Figure 8. UV-Visible spectra of mixture Mg, MB and Rh-B with base pH on NiAl-LDH (a), NiAl-HR (b), and HR (c)

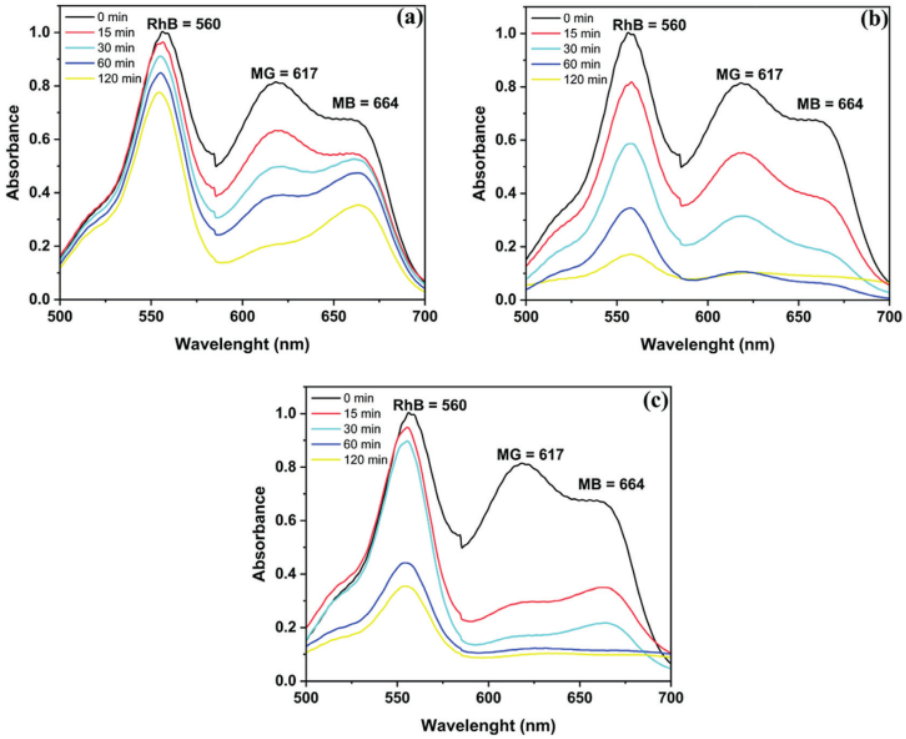

Figure 9. UV-Visible spectra of mixture Mg, MB and Rh-B with acid pH on NiAl-LDH (a), NiAl-HR (b), and HR (c)

The maximum wavelength of a mixture of malachite green, methylene blue and rhodamine-B dyes was measured in an acid pH using a UV-Vis spectrophotometer in the 500–700 nm wavelength range shown in Figure 9. The selectivity of adsorption to the dye mixture can be seen from changes in wavelength during adsorption. Under acidic conditions, it can be seen that for NiAl-LDH, HR and NiAl-HR adsorbents there is a decrease in absorbance after adsorption. Figure 9 shows that among the mixed dyes, more MG adsorbed as seen from the decrease in the absorbance value with the adsorption contact time and the adsorption concentration of MG at 120 minutes reached 98.263 mg/g for the NiAl-HR composite adsorbent.

CONCLUSIONS

In this study, the NiAl-HR composite material was successfully synthesized using the co-precipitation method and applied as an adsorbent to remove cationic dyes. NiAl-HR composite materials have a large adsorption capacity to adsorb cationic dyes. The adsorption follows the Langmuir adsorption isotherm model with the maximum capacity (Q_{max}) of the NiAl-HR composite material of 256.410 mg/g for MG and the adsorption process takes place spontaneously and endothermically. The regeneration process of NiAl-HR composites was more stable and the decrease was not significant (>70%). The selectivity of the dye mixture showed that the adsorbent was more selective for MG dye compared to MB and Rh-B.

Acknowledgement

This research is supported by the Ministry of Education and Culture of the Republic of Indonesia from the PDUPT Professional Grant 2021-2022 contact No.150/SP2H/LT/DRPM/2021. Special thanks to the Laboratory of Inorganic Materials and Complexes, Faculty of Mathematics and Natural Sciences, Sriwijaya University.

REFERENCES

1. Ahmed, D.N., Naji, L.A., Faisal, A.A.H., Al-Ansari, N., & Naushad, M. 2020. Waste foundry sand/Mg-Fe-layered double hydroxides composite material for efficient removal of Congo red dye from aqueous solution. Scientific Reports, 10(1), 1–12. https://doi.org/10.1038/s41598-020-58866-y
2. Alagha, O., Manzar, M.S., Zubair, M., Anil, I., Mu'azu, N.D., & Qureshi, A. 2020. Comparative adsorptive removal of phosphate and nitrate from wastewater using biochar-MgAl LDH nanocomposites: Coexisting anions effect and mechanistic studies. Nanomaterials, 10(2), 1–15. https://doi.org/10.3390/nano10020336
3. Almoisheer, N., Alseroury, F.A., Kumar, R., Aslam, M., Barakat, M.A. 2019. Adsorption and anion exchange insight of indigo carmine onto CuAl-LDH/SWCNTs nanocomposite: kinetic, thermodynamic and isotherm analysis. RSC Advances, 9(1), 560–568. https://doi.org/10.1039/C8RA09562K
4. Badri, A F, Mohadi, R., Lesbani, A. 2021a. Adsorptive Capacity of Malachite Green onto Mg/M_3^+ (M_3^+=Al and Cr) LDHs. Global NEST JournalGlobal NEST: The International Journal, 23(1), 74–81. https://doi.org/10.30955/gnj.003443.
5. Badri, A.F., Siregar, P.M.S.B.N., Palapa, N.R., Mohadi, R., Mardiyanto, M., Lesbani, A. 2021b). Mg-Al/Biochar Composite with Stable Structure for Malachite Green Adsorption from Aqueous Solutions. Bulletin of Chemical Reaction Engineering & Catalysis, 16(1), 149–160. https://doi.org/10.9767/bcrec.16.1.10270.149-160
6. Dada, A.O., Adekola, F.A., & Odebunmi, E.O. 2017. Kinetics, mechanism, isotherm and thermodynamic studies of liquid phase adsorption of Pb^{2+} onto wood activated carbon supported zerovalent iron (WAC-ZVI) nanocomposite. Cogent Chemistry, 3(1), 1351653. https://doi.org/10.1080/23312009.2017.1351653
7. Dang, W., Zhang, J., Nie, H., Wang, F., Tang, X., Wu, N., Chen, Q., Wei, X., & Wang, R. 2020. Isotherms, thermodynamics and kinetics of methane-shale adsorption pair under supercritical condition: Implications for understanding the nature of shale gas adsorption process. Chemical Engineering Journal, 383, 123191. https://doi.org/10.1016/j.cej.2019.123191
8. Daud, M., Hai, A., Banat, F., Wazir, M.B., Habib, M., Bharath, G., & Al-Harthi, M.A. 2019. A review on the recent advances, challenges and future aspect of layered double hydroxides (LDH) – Containing hybrids as promising adsorbents for dyes removal. Journal of Molecular Liquids, 288, 110989. https://doi.org/10.1016/j.molliq.2019.110989
9. Elmoubarki, R., Mahjoubi, F.Z., Elhalil, A., Tounsadi, H., Abdennouri, M., Sadiq, M., Qourzal, S., Zouhri, A., & Barka, N. 2017. Ni/Fe and Mg/Fe layered double hydroxides and their calcined derivatives: Preparation, characterization and application on textile dyes removal. Journal of Materials Research and Technology, 6(3), 271–283. https://doi.org/10.1016/j.jmrt.2016.09.007
10. Hashem, A., Fletcher, A.J., Younis, H., Mauof, H., & Abou-Okeil, A. 2020. Adsorption of Pb(II) ions from contaminated water by 1,2,3,4-butanetetracarboxylic acid-modified microcrystalline cellulose: Isotherms, kinetics, and thermodynamic studies. International Journal of Biological Macromolecules, 164, 3193–3203. https://doi.org/10.1016/j.ijbiomac.2020.08.159
11. He, H., Zhang, N., Chen, N., Lei, Z., Shimizu, K., & Zhang, Z. 2019. Efficient phosphate removal from wastewater by MgAl-LDHs modified hydrochar derived from tobacco stalk. Bioresource Technology Reports, 8, 100348. https://doi.org/10.1016/j.biteb.2019.100348
12. Hidayati, N., Mohadi, R., Elfita, E., & Lesbani, A. 2020. Malachite Green Removal by Zn/Al-citrate LDHs in Aqueous Solution. Science and Technology Indonesia, 5(2), 59-61. DOI: 10.26554/sti.2020.5.2.59-61
13. Hu, H., Wageh, S., Al-Ghamdi, A.A., Yang, S., Tian, Z., Cheng, B., & Ho, W. 2020. NiFe-LDH nanosheet/carbon fiber nanocomposite with enhanced anionic dye adsorption performance. Applied Surface Science, 511(01), 145570. https://doi.org/10.1016/j.apsusc.2020.145570
14. Iryani, A., Nur, H., Santoso, M., & Hartanto, D. 2020. Adsorption study of rhodamine B and methylene blue dyes with ZSM-5 directly synthesized from Bangka Kaolin without organic template. Indonesian Journal of Chemistry, 20(1), 130–140. https://doi.org/10.22146/ijc.41369
15. Jiang, D. Bin, Jing, C., Yuan, Y., Feng, L., Liu, X., Dong, F., Dong, B., & Zhang, Y.X. 2019. 2D-2D growth of NiFe LDH nanoflakes on montmorillonite for cationic and anionic dye adsorption performance. Journal of Colloid and Interface Science, 54*0*, 398–409. https://doi.org/10.1016/j.jcis.2019.01.022
16. Kaykhaii, M., Sasani, M., & Marghzari, S. 2018. Removal of Dyes from the Environment by Adsorption Process. Chemical and Materials Engineering, 6(2), 31–35. https://doi.org/10.13189/cme.2018.060201
17. Lesbani, A., Palapa, N.R., Taher, T., Andreas, R., & Mohadi, R. 2020. Ni/Al Layered Double Hydroxide Intercalated with Keggin Ion [a-SiW12O40]4- for Iron(II) Removal in Aqueous Solution Aldes. Molekul, 15(3), 149–157.
18. Lesbani, A., Palapa, N.R., Sayeri, R.J., Taher, T., & Hidayati, N. 2021. High reusability of NiAl LDH / biochar composite in the removal methylene blue from aqueous solution. 21(2), 421–434. https://doi.org/10.22146/ijc.56955
19. Li, L., Cao, G., & Zhu, R. 2020. Adsorption of Cr(VI) from aqueous solution by a litchi shell-based adsorbent. Environmental Research, VI, 110356. https://doi.org/10.1016/j.envres.2020.110356

20. Li, Q., Tang, X., Sun, Y., Wang, Y., Long, Y., Jiang, J., & Xu, H. 2015. Removal of Rhodamine B from wastewater by modified Volvariella volvacea: Batch and column study. RSC Advances, 5(32), 25337–25347. https://doi.org/10.1039/c4ra17319h
21. Lv, X., Qin, X., Wang, K., Peng, Y., Wang, P., & Jiang, G. 2019. Nanoscale zero valent iron supported on MgAl-LDH-decorated reduced graphene oxide: Enhanced performance in Cr(VI) removal, mechanism and regeneration. Journal of Hazardous Materials, 373, 176–186. https://doi.org/10.1016/j.jhazmat.2019.03.091
22. Meili, L., Lins, P.V., Zanta, C.L.P.S., Soletti, J.I., Ribeiro, L.M.O., Dornelas, C.B., Silva, T.L., & Vieira, M.G.A. 2019. MgAl-LDH/Biochar composites for methylene blue removal by adsorption. Applied Clay Science, 168, 11–20. https://doi.org/10.1016/j.clay.2018.10.012
23. Mikif, L.A., Abdulhusain, N., Jalil, H.M., & Salman, J.M. 2018. Removal of Organic Matters from Domestic Wastewater by Using Adsorption Technique. Mesopotamia Environmental Journal, 4(4), 16–24. https://doi.org/10.31759/mej.2018.4.4.0016
24. Mrózek, O., Ecorchard, P., Vomáčka, P., Ederer, J., Smržová, D., Slušná, M.Š., Machálková, A., Nevoralová, M., & Beneš, H. 2019. Mg-Al-La LDH-$MnFe_2O_4$ hybrid material for facile removal of anionic dyes from aqueous solutions. Applied Clay Science, 169, 1–9. https://doi.org/10.1016/j.clay.2018.12.018
25. Neolaka, Y.A.B., Lawa, Y., Naat, J.N., Riwu, A.A. P., Iqbal, M., Darmokoesoemo, H., & Kusuma, H.S. 2020. The adsorption of Cr(VI) from water samples using graphene oxide-magnetic (GO-Fe_3O_4) synthesized from natural cellulose-based graphite (kusambi wood or Schleichera oleosa): Study of kinetics, isotherms and thermodynamics. Journal of Materials Research and Technology, 9(3), 6544–6556. https://doi.org/10.1016/j.jmrt.2020.04.040
26. Oliveira, E.I.S., Santos, J.B., Gonçalves, A.P.B., Mattedi, S., & José, N.M. 2016. Characterization of the rambutan peel fiber (*Nephelium lappaceum*) as a lignocellulosic material for technological applications. Chemical Engineering Transactions, 50, 391–396. https://doi.org/10.3303/CET1650066
27. Palapa, N.R., Taher, T., Mohadi, R., Rachmat, A., & Lesbani, A. 2021. Preparation of copper aluminum-biochar composite as adsorbent of malachite green in aqueous solution. Journal of Engineering Science and Technology, 16(1), 259-274. DOI: 10.21203/rs.3.rs-18799/v1
28. Palapa, N.R., Taher, T., Rahayu, B.R., & Mohadi, R. 2020. CuAl LDH/rice husk biochar composite for enhanced adsorptive removal of cationic dye from aqueous solution. 15(2), 525–537. https://doi.org/10.9767/bcrec.15.2.7828.525-537
29. Rathee, G., Awasthi, A., Sood, D., Tomar, R., Tomar, V., & Chandra, R. 2019. A new biocompatible ternary layered double hydroxide adsorbent for ultrafast removal of anionic organic dyes. Scientific Reports, 9(1), 1–14. https://doi.org/10.1038/s41598-019-52849-4
30. Razak, A.A., & Rohani, S. 2018. Sodium dodecyl sulfate-modified Fe_2O_3/molecular sieves for removal of rhodamine B dyes. Advances in Materials Science and Engineering, 2018. https://doi.org/10.1155/2018/3849867
31. Saghir, S., Fu, E., & Xiao, Z. 2020. Synthesis of CoCu-LDH nanosheets derived from zeolitic imidazole framework-67 (ZIF-67) as an efficient adsorbent for azo dye from waste water. Microporous and Mesoporous Materials, 297. https://doi.org/10.1016/j.micromeso.2020.110010
32. Shan, R.R., Yan, L.G., Yang, K., Yu, S.J., Hao, Y.F., Yu, H. Q., & Du, B. 2014. Magnetic Fe3O4/MgAl-LDH composite for effective removal of three red dyes from aqueous solution. Chemical Engineering Journal, 252, 38–46. https://doi.org/10.1016/j.cej.2014.04.105
33. Srivatsav, P., Bhargav, B.S., Shanmugasundaram, V., Arun, J., Gopinath, K.P., & Bhatnagar, A. 2020. Biochar as an eco-friendly and economical adsorbent for the removal of colorants (Dyes) from aqueous environment: A review. Water (Switzerland), 12(12), 1–27. https://doi.org/10.3390/w12123561
34. Siregar, P.M.S.B.N., Palapa, N.R., Wijaya, A., Fitri, E.S., & Lesbani, A. 2021. Structural stability of Ni/Al layered double hydroxide supported on graphite and biochar toward adsorption of congo red. Science and Technology Indonesia, 6(2), 85-95. DOI: 10.26554/sti.2021.6.2.85-95
35. Stawiński, W., Węgrzyn, A., Mordarski, G., Skiba, M., Freitas, O., & Figueiredo, S. 2018. Sustainable adsorbents formed from by-product of acid activation of vermiculite and leached-vermiculite-LDH hybrids for removal of industrial dyes and metal cations. Applied Clay Science, 161, 6–14. https://doi.org/10.1016/j.clay.2018.04.007
36. Tcheumi, H.L., Kameni Wendji, A.P., Tonle, I. K., & Ngameni, E. 2020. A low-cost layered double hydroxide (LDH) based amperometric sensor for the detection of isoproturon in water using carbon paste modified electrode. Journal of Analytical Methods in Chemistry. https://doi.org/10.1155/2020/8068137
37. Wang, Y., & Zhang, L. 2020. Improved performance of 3D hierarchical NiAl-LDHs micro-flowers via a surface anchored ZIF-8 for rapid multiple-pollutants simultaneous removal and residues monitoring. Journal of Hazardous Materials, 395, 122635. https://doi.org/10.1016/j.jhazmat.2020.122635
38. Zhang, M., Gao, B., Fang, J., Creamer, A.E., & Ullman, J.L. 2014. Self-assembly of needle-like layered double hydroxide (LDH) nanocrystals on hydrochar: Characterization and phosphate removal ability. RSC Advances, 4(53), 28171–28175. https://doi.org/10.1039/c4ra02332c
39. Zhu, Z., Xiang, M., Li, P., Shan, L., & Zhang, P. 2020. Surfactant-modified three-dimensional layered double hydroxide for the removal of methyl orange and rhodamine B: Extended investigations in binary dye systems. Journal of Solid State Chemistry, 288. https://doi.org/10.1016/j.jssc.2020.121448

C.1.c.2.5-Competitive Removal of Cationic Dye Using NiAl-LDH.pdf

ORIGINALITY REPORT

10%
SIMILARITY INDEX

PRIMARY SOURCES

1	journal.ugm.ac.id Internet	93 words —	2%
2	www.infona.pl Internet	84 words —	2%
3	sciencetechindonesia.com Internet	70 words —	1%
4	cst.kipmi.or.id Internet	59 words —	1%
5	www.hindawi.com Internet	43 words —	1%
6	res.mdpi.com Internet	39 words —	1%
7	www.jett.dormaj.com Internet	36 words —	1%
8	www.sciencetechindonesia.com Internet	36 words —	1%
9	ijstr.org Internet	32 words —	1%

EXCLUDE QUOTES	OFF	EXCLUDE MATCHES	< 1%
EXCLUDE BIBLIOGRAPHY	ON		